A gut bacterial amyloid promotes α-synuclein aggregation and motor impairment in mice

Timothy R Sampson[1‡*], Collin Challis[1†], Neha Jain[2†§], Anastasiya Moiseyenko[1], Mark S Ladinsky[1], Gauri G Shastri[1], Taren Thron[1], Brittany D Needham[1], Istvan Horvath[3], Justine W Debelius[4#], Stefan Janssen[4¶], Rob Knight[4,5], Pernilla Wittung-Stafshede[3], Viviana Gradinaru[1], Matthew Chapman[2], Sarkis K Mazmanian[1*]

[1]Division of Biology & Biological Engineering, California Institute of Technology, Pasadena, United States; [2]Department of Molecular, Cellular, and Developmental Biology, University of Michigan, Ann Arbor, United States; [3]Department of Biology and Biological Engineering, Chalmers University of Technology, Gothenburg, Sweden; [4]Department of Pediatrics, University of California, San Diego, San Diego, United States; [5]Department of Computer Science and Engineering, University of California, San Diego, San Diego, United States

*For correspondence:
trsamps@emory.edu (TRS);
sarkis@caltech.edu (SKM)

[†]These authors contributed equally to this work

Present address: [‡]Department of Physiology, Emory University School of Medicine, Atlanta, United States; [§]Department of Bioscience and Bioengineering, Indian Institute of Technology, Jodhpur, India; [#]Department of Microbiology, Tumor and Cell Biology, Karolinska Institutet, Stockholm, Sweden; [¶]Algorithmic Bioinformatics, Justus-Liebig-University Giessen, Giessen, Germany

Abstract Amyloids are a class of protein with unique self-aggregation properties, and their aberrant accumulation can lead to cellular dysfunctions associated with neurodegenerative diseases. While genetic and environmental factors can influence amyloid formation, molecular triggers and/or facilitators are not well defined. Growing evidence suggests that non-identical amyloid proteins may accelerate reciprocal amyloid aggregation in a prion-like fashion. While humans encode ~30 amyloidogenic proteins, the gut microbiome also produces functional amyloids. For example, curli are cell surface amyloid proteins abundantly expressed by certain gut bacteria. In mice overexpressing the human amyloid α-synuclein (αSyn), we reveal that colonization with curli-producing *Escherichia coli* promotes αSyn pathology in the gut and the brain. Curli expression is required for *E. coli* to exacerbate αSyn-induced behavioral deficits, including intestinal and motor impairments. Purified curli subunits accelerate αSyn aggregation in biochemical assays, while oral treatment of mice with a gut-restricted amyloid inhibitor prevents curli-mediated acceleration of pathology and behavioral abnormalities. We propose that exposure to microbial amyloids in the gastrointestinal tract can accelerate αSyn aggregation and disease in the gut and the brain.

Introduction

The accumulation and aggregation of amyloid proteins occurs during many neurodegenerative diseases. Synucleinopathies are one family of amyloid disease, which includes Parkinson's disease (PD), Lewy Body disease (LBD), and Multiple System Atrophy (MSA). Central to their pathogenesis is the accumulation of the neuronal protein α-Synuclein (αSyn) into insoluble amyloid aggregations, which ultimately leads to inflammation and neuronal dysfunction (*Jucker and Walker, 2013*; *Brettschneider et al., 2015*). αSyn aggregation can contribute to the death of dopaminergic neurons in specific brain regions, resulting in motor symptoms (*Poewe et al., 2017*). Clinical and epidemiological data suggest that accumulation of αSyn aggregates may first occur at peripheral sites, such as the olfactory epithelium or gastrointestinal (GI) tract, before spreading to the brain (*Braak et al., 2003*). Individuals diagnosed with various synucleinopathies often display constipation

and other GI dysfunctions years prior to the onset of movement dysfunction (*Verbaan et al., 2007*; *Colosimo, 2011*; *Engen et al., 2017*; *Mertsalmi et al., 2017*; *Sakakibara et al., 2019*). Experimental evidence exists for a prion-like spread of αSyn aggregates (*Woerman et al., 2015*), including propagation from the gut to the brain via the vagus nerve and/or spinal cord in rodent models (*Holmqvist et al., 2014*; *Uemura et al., 2018*; *Van Den Berge et al., 2019*). In humans, recent epidemiological studies suggest an association between truncal vagotomy and appendectomy with a decreased risk of PD (*Svensson et al., 2015*; *Liu et al., 2017*; *Killinger et al., 2018*), and in increased risk of comorbidity with inflammatory bowel disease (IBD) (*Hui et al., 2018*; *Peter et al., 2018*). While a role for protein aggregation and/or inflammation in the gut represents an emerging area of research in synucleinopathies, the GI tract has been implicated in other neurological disorders such as autism spectrum disorder, depression, anxiety and Alzheimer's disease (*Vuong et al., 2017*).

The gut is colonized with a complex microbiome that impacts development and function of the immune, metabolic and nervous systems (*Fung et al., 2017*). Enterobacteriaceae, highly prevalent within the gut of humans, can produce functional amyloid proteins termed curli (*Tursi and Tükel, 2018*). Curli fibers are formed by bacterial secretion of an unfolded amyloid, CsgA, that subsequently aggregates extracellularly to form biofilms, mediate adhesion to epithelial cells, and are involved in bacteriophage defense (*Tursi and Tükel, 2018*; *Vidakovic et al., 2018*). Exposure to curli not only modulates host inflammatory responses within the intestinal tract and periphery (*Gallo et al., 2015*; *Chen et al., 2016*; *Tursi and Tükel, 2018*), but oral administration of curli-producing bacteria can also increase production and aggregation of the amyloid protein αSyn in aged rats and nematodes (*Chen et al., 2016*). Biochemical studies demonstrate that native, bacterial chaperones of curli are capable of transiently interacting with αSyn and modulating its aggregation (*Chorell et al., 2015*; *Evans et al., 2015*). Interestingly, diverse human amyloid proteins including αSyn, amyloid beta (Aβ), cellular prion protein (PrP^C), and Tau can accelerate the amyloidogenesis of heterologous mammalian amyloid proteins (*Clinton et al., 2010*; *Brettschneider et al., 2015*; *Katorcha et al., 2017*). Lesions containing mixed human amyloids have been observed in neurodegenerative brains (*Rahimi and Kovacs, 2014*; *Spires-Jones et al., 2017*), implicating interactions between different amyloidogenic proteins in resulting pathology. Accordingly, we wondered whether a bacterial amyloid protein can contribute to heterologous aggregation of mammalian αSyn in the gut and the brain, leading to synucleinopathy-related behaviors.

Herein, we reveal that mono-colonization of αSyn-overexpressing mice with curli-producing *Escherichia coli* exacerbates motor impairment and GI dysfunction, and promotes αSyn aggregation and inflammation in the gut and brain. Enrichment of curli-producing *E. coli* to mice harboring a healthy human microbiome is sufficient to aggravate αSyn-dependent pathophysiology. The purified amyloidogenic subunit of curli fibers (CsgA) is sufficient to accelerate αSyn aggregation during in vitro biochemical assays and pathophysiology in mice following intra-intestinal administration, while variants of CsgA that are unable to form amyloids have no effect on αSyn aggregation. Oral treatment of mice with a gut-restricted amyloid inhibitor reduces *csgA* expression in the gut, limits αSyn aggregation in the brain, and alleviates GI and motor deficits in mice that overexpress αSyn. These data provide novel insights into a trans-kingdom interaction between the gut microbiome and mammalian amyloids, and suggest the possibility that carriage of particular bacterial taxa may be a factor that can exacerbate neurologic disease.

Results and discussion

Mono-colonization with curli-producing gut bacteria enhances αSyn pathophysiology

We previously identified that depletion of the microbiome reduces pathophysiology in Thy1-αSyn mice (alpha-synuclein overexpressing; ASO mice) (*Sampson et al., 2016*), which overexpress wild-type human αSyn. Due to accumulation and aggregation of neuronal αSyn, mice display increased neuroinflammation, GI dysfunction, and progressive motor abnormalities (*Rockenstein et al., 2002*; *Chesselet et al., 2012*; *Wang et al., 2012*) that are relevant in the study of synucleinopathies. Prior findings in germ-free Thy1-αSyn mice suggest that an unidentified member(s) of the gut microbiome may be pathogenic in this mouse model (*Sampson et al., 2016*). Interestingly, increased colonization

and mucosal association with Enterobacteriaceae, such as *E. coli*, have been reported in individuals with PD compared to healthy controls (*Forsyth et al., 2011*), as well as a positive association of Enterobacteriaceae abundance with disease severity (*Scheperjans et al., 2015*; *Li et al., 2017*).

To establish whether *E. coli* promotes αSyn-dependent motor dysfunction, we mono-associated germ-free (GF) wild-type and ASO mice with the curli-producing *E. coli* strain MC4100, or *Bacteroides fragilis* strain NCTC9343 and segmented filamentous bacteria (SFB), which do not produce curli. *E. coli* exacerbated the αSyn-dependent motor defects in ASO animals across a battery of tests, compared to the other taxa (*Figure 1A–F* and *Figure 1—figure supplement 1A–E*). To determine the contribution of curli amyloids, we compared mice mono-colonized with wild-type *E. coli* (WT) to those mono-colonized with an isogenic mutant lacking genes encoding the curli biosynthesis machinery (Δ*csgBAC*) (*Wang and Chapman, 2008*). Evaluation of coordinated motor function revealed that colonization with the curli-deficient strain did not elicit robust motor impairment (*Figure 1A–F*). We did not observe curli-dependent alterations to colonization levels or mucosal association, despite detecting *csgA* expression (*Figure 1—figure supplement 1F–I*). In addition, the curli-deficient mutant did not display alterations to lipopolysaccharide potency or structure (*Figure 1—figure supplement 1J,K*). Thus, curli-producing bacteria are capable of enhancing motor deficits in ASO mice.

ASO mice colonized with curli-producing bacteria displayed increased αSyn fibril reactivity and detergent-insoluble αSyn in the midbrain compared to mice with the Δ*csgBAC* strain, despite similar transgene production (*Figure 1—figure supplement 2A–D,F,G*). Histological and western blot analysis revealed increased phospho-serine129 αSyn (pS129-αSyn) deposition in the substantia nigra (SN) of ASO mice, indicative of pathological αSyn aggregation, (*Figure 1G,H*, and *Figure 1—figure supplement 2E,H,J*). Further, mice colonized with WT *E. coli* show increased proteinase K-resistant αSyn inclusions in the midbrain (*Figure 1I* and *Figure 1—figure supplement 2I*), with little alteration to pS129-αSyn in the frontal cortex (*Figure 1—figure supplement 2K,L*). Additionally, we observed increased pS129-αSyn in the proximal large intestine, and elevated αSyn fibril reactivity in the duodenum and proximal large intestine of ASO mice mono-colonized with curli-producing *E. coli* (*Figure 1—figure supplement 2M–P*). Previous research has shown that synuclein pathology, neuroinflammation, and motor defects occur at early ages in the ASO mouse model without concomitant loss of striatal dopamine, tyrosine hydroxylase positive (TH^{+}) neurons in the midbrain, or loss of neurons in the myenteric plexus (*Fleming et al., 2004*; *Lam et al., 2011*; *Chesselet et al., 2012*; *Wang et al., 2012*). Consistent with these prior observations, we do not observe decreases in total striatal dopamine, midbrain *TH* expression, TH^{+} neurons, nor myenteric PGP9.5^{+} neurons, under the colonization conditions and ages assessed, suggesting pathology and motor deficits are independent of dopamine or neuron loss (*Figure 1*, figure supplement S2Q-S).

Mono-colonization of ASO mice with curli-producing *E. coli* resulted in increased expression of the proinflammatory cytokines interleukin 6 (IL-6) and tumor necrosis factor alpha (TNFα) in brain-derived CD11b^{+} cells, and increased cytokine production in the midbrain and striatum (*Figure 1—figure supplement 3A–C*). In addition, Iba^{+} microglia morphologies indicated reduced activation in ASO mice colonized with the curli-deficient strain (*Figure 1—figure supplement 3D–G*). Multiplexed ELISA analysis revealed increased cytokine and chemokine production in colonic tissue of mice mono-colonized with curli-producing *E. coli*, irrespective of genotype (*Figure 1—figure supplement 3H,J,K*), and no noteworthy changes to serum cytokines of ASO mice based on colonization status (*Figure 1—figure supplement 3I*). These data reveal that a bacterial amyloid from the gut microbiome can exacerbate pathology and inflammation, in both the gut and brain, in mice that overexpress αSyn.

Curli biosynthesis within a complex microbiome contributes to motor and GI deficits

To explore host-microbiome interactions in a more natural context, we tested whether introduction of curli-producing bacteria to a healthy human microbiota is sufficient to enhance αSyn-dependent pathophysiology. GF ASO mice were transplanted with fecal microbiota from a human donor predicted to contain low levels of *csgA*, as indicated by PICRUSt analysis following 16S rRNA sequencing (*Figure 2—figure supplement 1A*). This single microbiome was supplemented with either WT *E. coli* or the Δ*csgBAC* strain. Both strains reached similar abundances in the feces (*Figure 2—figure supplement 1B,C*), while *csgA* expression and amyloid production appeared only in mice colonized
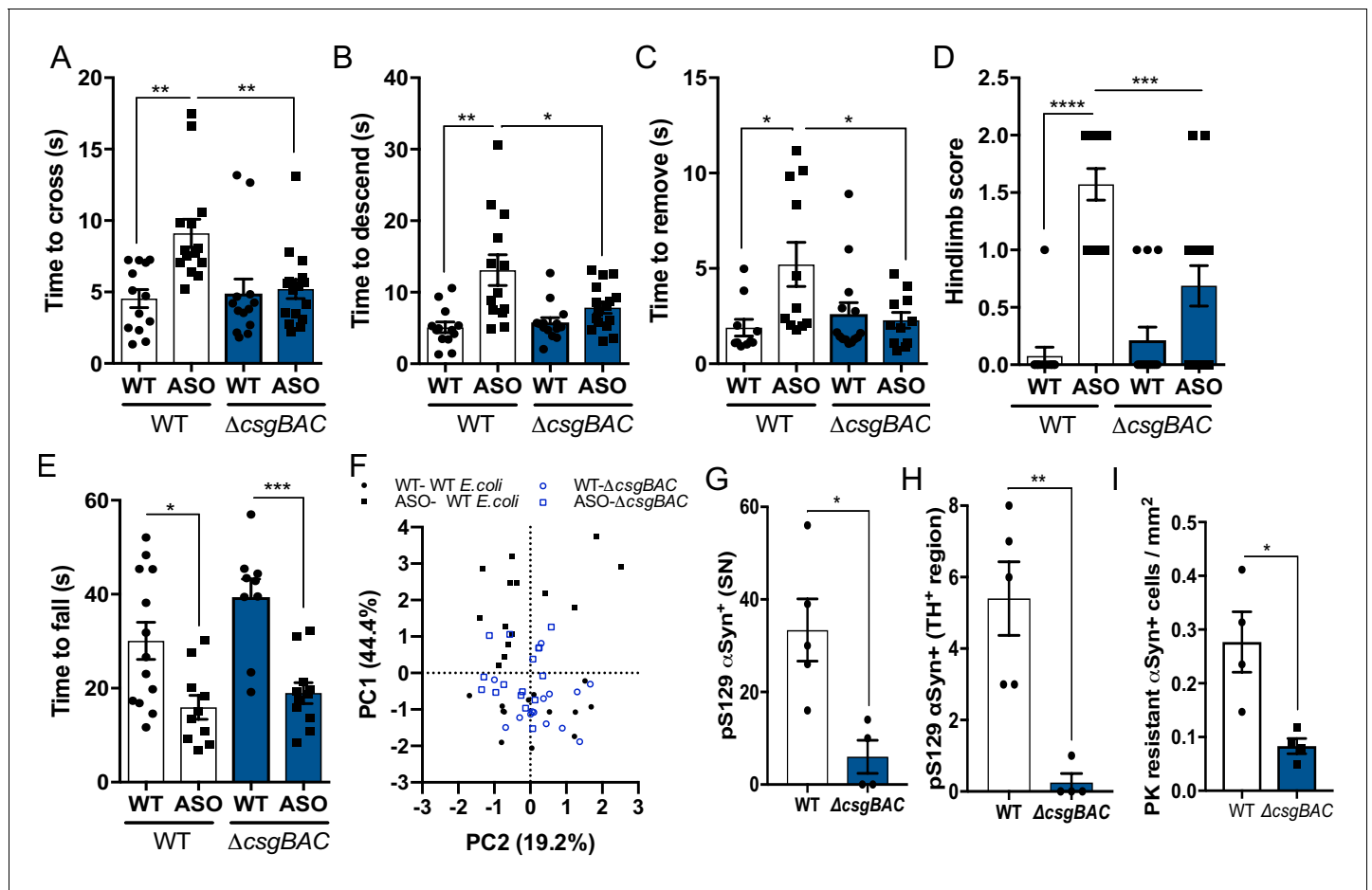
Figure 1. Mono-colonization with curli-producing gut bacteria enhances αSyn pathophysiology germ-free wild-type BDF1 (WT) and Thy1-αSyn (ASO) mice were mono-colonized with wild-type *E. coli* MC4100 (WT) or an isogenic curli-deficient strain (Δ*csgBAC*) at 5–6 weeks of age. Motor function was assessed at 12–13 weeks of age by quantifying (A), beam traversal time, (B), pole descent time, (C), nasal adhesive removal time, (D), hindlimb clasping score, (E), wirehang time. (F), Principal component analysis of compiled motor scores from tests in (A–E). Quantification of (G, H) pS129αSyn and (I) proteinase K–resistant αSyn by immunofluorescence microscopy in the substantia nigra and midbrain. n = 13–16 (A–F), n = 4.5 (G–I). Points represent individuals, bars represent the mean and standard error. Data analyzed by one-way ANOVA with Tukey post-hoc test (A–E), and two-tailed *t*-test for (G–I). *p≤0.05; **p≤0.01; ***p≤0.001; ****p≤0.0001. Motor data are compiled from three independent cohorts.

The online version of this article includes the following source data and figure supplement(s) for figure 1:

Source data 1. Source data and statistical analysis.

Figure supplement 1. *E. coli* alters motor deficits, and CsgA does not influence colonization, inflammatory capacity, or dopamine production Germ-free (GF) wild-type (WT) or Thy1- αSyn (ASO) mice were mono-colonized with either *Bacteroides fragilis* (Bfrag), segmented filamentous bacteria (SFB), or *Escherichia coli* (Ecoli).

Figure supplement 1—source data 1. Source data and statistical analysis.

Figure supplement 2. Mono-colonization with curli-sufficient bacteria induce increased αSyn-dependent pathology Germ-free (GF) wild-type (WT) or Thy1-αSyn (ASO) animals were mono-colonized with curli-sufficient *E. coli* (WT) or curli-deficient *E. coli* (Δ*csgBAC*).

Figure supplement 2—source data 1. Source data and statistical analysis.

Figure supplement 3. Mono-colonization with curli-sufficient bacteria induces altered inflammatory responses in the brain and intestine.

Figure supplement 3—source data 1. Source data and statistical analysis.

with WT bacteria (*Figure 2—figure supplement 1C–E*). Mice harboring a microbiota containing WT *E. coli* displayed significantly impaired motor and GI performance compared to animals with a complex microbiota plus the curli-deficient strain (*Figure 2A–G*). Moreover, enrichment of curli-producing bacteria resulted in increased αSyn fibril reactivity in the midbrain and elevated pS129-αSyn deposition in the SN, without changes to the number of TH+ neurons (*Figure 2H* and *Figure 2—figure supplement 1F–J*). Morphometric analysis of microglia demonstrated concomitant changes
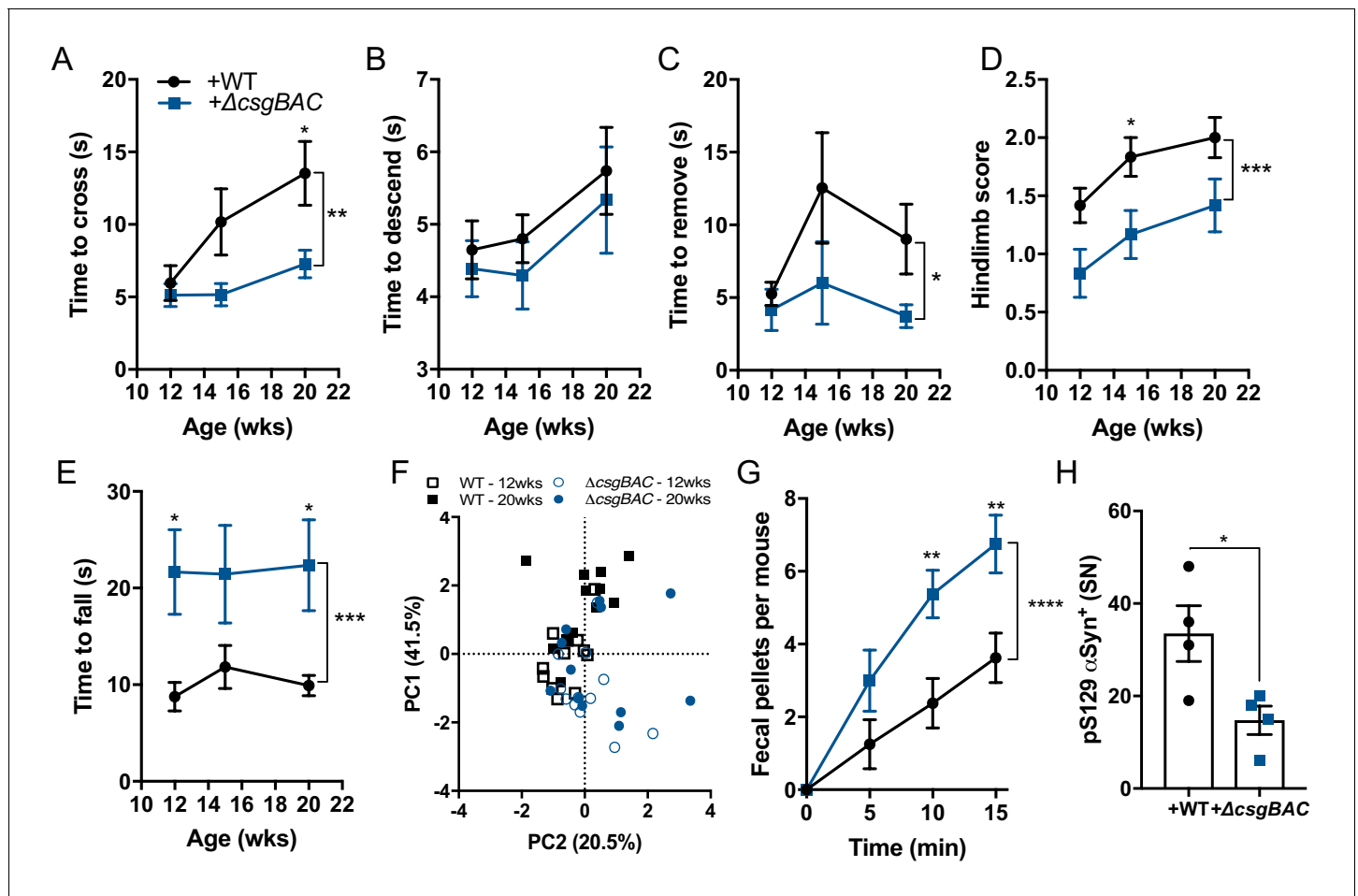
Figure 2. Curli biosynthesis within a complex microbiome contributes to motor and GI deficits Germ-free Thy1-αSyn (ASO) mice were colonized with fecal microbes derived from healthy human at 5–6 weeks of age, and concurrently supplemented with either wild-type *E. coli* MC4100 (+WT) or a curli-deficient strain (+ΔcsgBAC). Motor function was tested longitudinally at 12, 15, and 20 weeks of age in the (A) beam traversal, (B) pole descent, (C) adhesive removal, (D) hindlimb clasping score, (E) wirehang tests. (F) Principal component analysis of compiled motor scores from tests in (A–E). (G) Fecal output over a 15-min period observed at week 21 of age. Quantification of (H) pS129αSyn by immunofluorescence microscopy in the substantia nigra. n = 12 (A–F), n = 6 (G), n = 4 (H). Data points represent individuals, bars represent the mean and standard error. Time courses analyzed by two-way ANOVA, with Sidak post-hoc test for between group comparisons indicated above individual time points, and brackets indicating significance between colonization status. Data in (H) analyzed two-tailed *t*-test. *p≤0.05; **p≤0.01; ***p≤0.001; ****p≤0.0001. Motor data are compiled from two independent cohorts.

The online version of this article includes the following source data and figure supplement(s) for figure 2:

Source data 1. Source data and statistical analysis.

Figure supplement 1. Amyloid-producing bacteria in humanized animals modulate microglia responses.

Figure supplement 1—source data 1. Source data and statistical analysis.

---

indicative of inflammatory status in the midbrain (*Figure 2—figure supplement 1K–N*). Therefore, in the context of a complex human microbiota, curli-producing *E. coli* are sufficient to modulate αSyn-mediated pathophysiology.

The bacterial amyloid protein, CsgA, accelerates αSyn fibrilization

Emerging data suggest that non-orthologous amyloid proteins can accelerate heterologous aggregation (*Clinton et al., 2010*; *Brettschneider et al., 2015*; *Katorcha et al., 2017*). We therefore tested whether CsgA can directly impact aggregation of αSyn. Purified monomeric CsgA accelerated production of αSyn aggregates during in vitro biochemical amyloid assays (*Figure 3A–C* and *Figure 3—figure supplement 1A*), even at concentrations below which CsgA self-aggregates
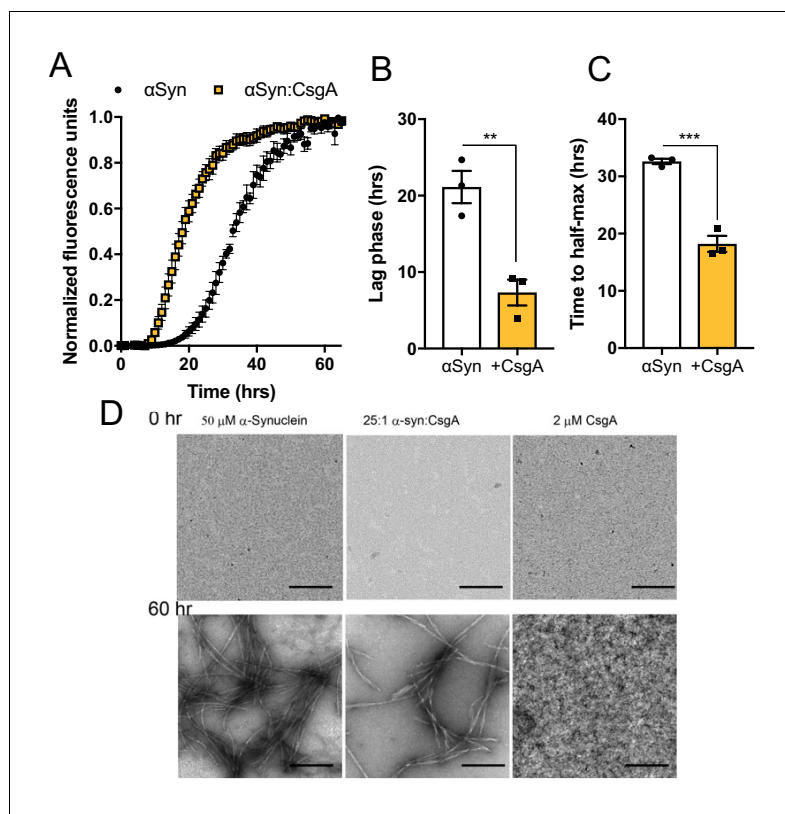
Figure 3. The bacterial amyloid protein, CsgA, accelerates αSyn fibrilization In vitro biophysical analysis with purified αSyn and CsgA proteins. (**A**) Aggregation as measured by Thioflavin T fluorescence over time during αSyn amyloid formation alone or in the presence of CsgA monomers (25:1 molar ratio). Time to reach (**B**) exponential fibrilization/lag phase and (**C**) half-maximum from reactions in (**A**). (**D**) Representative transmission electron micrographs of αSyn or CsgA alone, or in combination, at 0 and 60 hr post-aggregation. n = 3 (**A–C**). Bars represent the mean and standard error. Data are analyzed by two-tailed, *t*-test. **p≤0.01; ***p≤0.001.
The online version of this article includes the following source data and figure supplement(s) for figure 3:

Source data 1. Source data and statistical analysis.
Figure supplement 1. CsgA seeds αSyn aggregation and propagation in vitro.
Figure supplement 1—source data 1. Source data and statistical analysis.
Figure supplement 2. CsgA seeds αSyn aggregation in vitro and in vivo through native amyloidogenic properties.
Figure supplement 2—source data 1. Source data and statistical analysis.
Figure supplement 3. Intestinal injection of amyloidogenic curli promotes progressive motor dysfunction.
Figure supplement 3—source data 1. Source data and statistical analysis.

(*Figure 3D*). The αSyn fibrils purified from these reactions maintained an ability to accelerate αSyn amyloidogenesis (*Figure 3—figure supplement 1B,C*), suggesting that CsgA-induced αSyn aggregates are propagation-competent, similar to other amyloids (*Spires-Jones et al., 2017*). Surprisingly, we could not detect a direct interaction between purified CsgA and αSyn monomers by surface plasmon resonance (*Figure 3—figure supplement 1D*), perhaps indicating transient interactions or requirements for prior oligomerization of either or both proteins. Unlike αSyn, Tau aggregation was not accelerated by CsgA (*Figure 3—figure supplement 1E–G*). Native amyloid-forming properties of CsgA are required, as a non-amyloidogenic form of CsgA (CsgA:Q49A/N54A/Q139A/N144A; 'SlowGo' *Wang and Chapman, 2008*) did not augment αSyn aggregation in vitro (*Figure 3—figure supplement 2A–C*). To investigate the dependence of these amyloidogenic residues in vivo, we mono-colonized ASO mice with *E. coli* producing either wild-type CsgA or CsgA:SlowGo proteins (*Wang and Chapman, 2008*). Motor performance in ASO mice harboring SlowGo-producing *E. coli* was less severe in comparison to mice colonized with WT bacteria (*Figure 3—figure supplement 2D–H*), although not to the extent of the ΔcsgBAC strain, qualitatively (see *Figure 1*).

Next, a peptide spanning the aggregation domain of CsgA or a non-amyloidogenic version (N122A) (*Tükel et al., 2009*) were injected directly into the intestinal wall of SPF ASO mice. Intra-intestinal delivery of amyloidogenic CsgA peptide, but not the mutant peptide, resulted in progressive motor and GI dysfunction (*Figure 3—figure supplement 3A–G*). Furthermore, increased αSyn fibrils were detected in the midbrains of amyloidogenic peptide-injected animals (*Figure 3—figure supplement 3H*). We conclude that gut exposure to a bacterial amyloid is sufficient to exacerbate motor deficits and αSyn brain pathology in this mouse model, in a manner dependent on CsgA aggregation.

Curli-driven pathophysiology in mice requires functional amyloid formation

Epigallocatechin gallate (EGCG) is a plant-derived, dietary polyphenol that physically inhibits amyloid formation, including αSyn aggregation (*Bieschke et al., 2010*). EGCG is also capable of blocking CsgA amyloidogenesis and represses *csgA* transcript expression in *E. coli* through activation of specific stress response pathways within the bacterial cell (*Serra et al., 2016*). We reveal here that EGCG treatment did not impair *E. coli* growth in culture, but significantly reduced biofilm formation, a process dependent on the production and assembly of curli (*Figure 4—figure supplement 1A, B*) (*Tursi and Tükel, 2018*). Additionally, EGCG also inhibited CsgA-accelerated αSyn amyloid formation during in vitro biochemical aggregation assays (*Figure 4A*). Notably, EGCG remains largely gut-restricted in rodents and humans and is not readily bioavailable in circulation or brain tissues following oral administration (*Lambert et al., 2003*; *Lin et al., 2007*; *Cai et al., 2018*). Oral treatment of wild-type *E. coli* mono-colonized ASO mice with EGCG did not affect fecal *E. coli* abundance, but resulted in decreased *csgA* production (*Figure 4B* and *Figure 4—figure supplement 1C*). Assessment of motor performance revealed that EGCG improved both motor and GI defects exacerbated by curli-producing *E. coli* in ASO mice (*Figure 4C–I* and *Figure 4—figure supplement 1D–I*). In addition, oral EGCG administration reduced αSyn aggregation and pS129-αSyn deposition in both the striatum and midbrain (*Figure 4J* and *Figure 4—figure supplement 1J–M*). Furthermore, microglia morphological changes were limited in EGCG-treated mice (*Figure 4—figure supplement 1O–R*). In addition to its ability to directly inhibit aggregation of bacterial and host-derived amyloids, EGCG has antioxidant and anti-inflammatory activities (*Li et al., 2004*) that may also contribute to the rescue of CsgA-accelerated, αSyn-dependent pathophysiology. Collectively, these data reveal that curli is a specific bacterial structure that can accelerate mammalian amyloid aggregation in vitro and in vivo.

Conclusion

The majority of synucleinopathy incidences are idiopathic, with multifactorial and complex risks that contribute to disease initiation and/or progression (*Ritz et al., 2016*; *Soldner et al., 2016*; *Johnson et al., 2019*). Our findings reveal that the bacterial amyloid CsgA can accelerate αSyn aggregation and enhance motor abnormalities in mice that are genetically predisposed to αSyn pathology. Curli production in the gut of non-susceptible mice does not impair motor performance at the timepoints examined, suggesting that this microbial trigger is not sufficient, but rather requires additional predisposing factors to promote disease outcomes. Further, inhibiting amyloid formation in the gut correlates with improvements in curli-induced behaviors and pathology. Our study does not reconcile how curli production within the gastrointestinal tract ultimately manifests αSyn aggregation in the brain. Experimental evidence exists for a prion-like spread of αSyn aggregates (*Woerman et al., 2015*), including propagation from the gut to the midbrain via the vagus nerve and/or spinal cord in rodent models (*Uemura et al., 2018*; *Kim et al., 2019*; *Van Den Berge et al., 2019*), although evidence for sustained propagation from the GI tract to structures outside the brainstem in primates is currently lacking (*Manfredsson et al., 2018*). Epidemiological studies suggest an association between full truncal vagotomy with a decreased risk of PD (*Svensson et al., 2015*). Intriguingly, there appears to be a positive correlation between inflammatory bowel disease and neurodegenerative disease (*Hui et al., 2018*; *Peter et al., 2018*). In experimental models, induction of GI inflammation, for instance through LPS or dextran sodium sulfate administration, is sufficient to induce αSyn pathology in the CNS (*Choi et al., 2018*; *Kishimoto et al., 2019*; *Perez-Pardo et al., 2019*). Aggregates of both CsgA and αSyn are capable of signaling through the innate
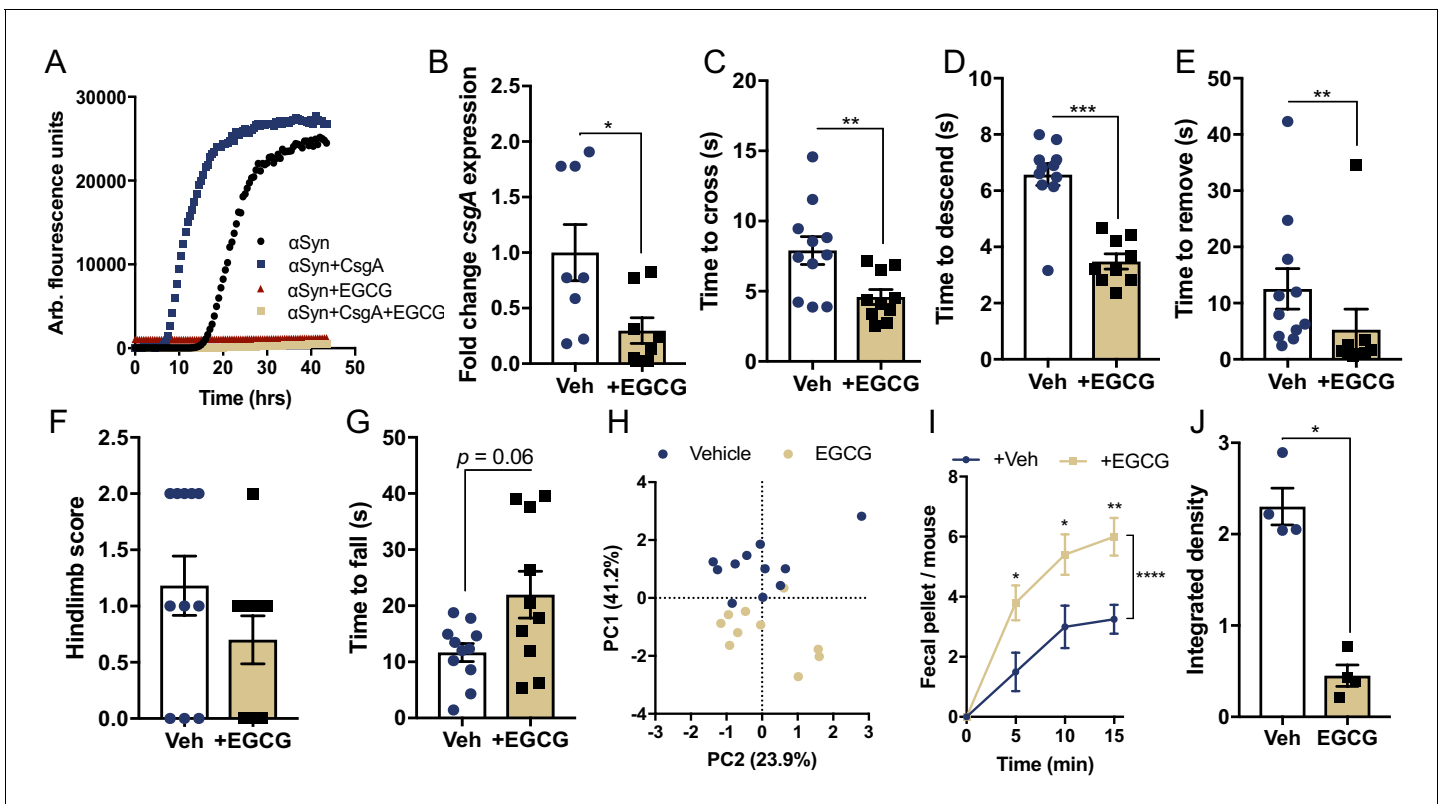
Figure 4. Curli-driven pathophysiology in mice requires functional amyloid formation. (**A**), Representative in vitro αSyn aggregation measured by Thioflavin T fluorescence during αSyn amyloid formation alone or in the presence of CsgA (25:1 molar ratio), with and without EGCG (50 μM) treatment. (**B–H**) Germ-free Thy1-αSyn mice (ASO) were mono-colonized with WT *E. coli* at 5–6 weeks of age, and given water alone (Vehicle: Veh) or treated with EGCG *ad lib* in drinking water (+EGCG). (**B**) RNA was extracted from fecal pellets and *csgA* expression quantified by qRT-PCR, relative to *rrsA*. Motor function was assessed at 15–16 weeks of age by quantifying (**C**) beam traversal time, (**D**) pole descent time, (**E**) nasal adhesive removal time, (**F**) hindlimb clasping score, (**G**) wirehang tests. (**H**) Principal component analysis of compiled motor scores from tests in (**C–G**). (**I**) Fecal output over a 15 min period. (**J**) Quantification of insoluble αSyn fibrils in the ventral midbrain by dot blot assay. n = 8 (**B**); n = 10–11 (**C–G**); n = 4–5 (**I, J**). Points represent individuals, bars represent the mean and standard error. Data analyzed by two-tailed Mann-Whitney for **B–G**, (**J**) and two-way ANOVA with Sidek's post-hoc test for **I** with between group comparisons indicated above individual time points, and brackets indicating significance between treatment status. *$p \le 0.05$; **$p \le 0.01$; ***$p \le 0.001$; ****$p \le 0.0001$. Motor data compiled from two independent cohorts.

The online version of this article includes the following source data and figure supplement(s) for figure 4:

Source data 1. Source data and statistical analysis.

Figure supplement 1. Inhibition of functional amyloid formation dampens progressive pathophysiology.

Figure supplement 1—source data 1. Source data and statistical analysis.

immune receptor Toll-like receptor 2 (TLR2) leading to increased inflammatory responses (*Tükel et al., 2009*; *Poewe et al., 2017*). In fact, inhibiting TLR2 in αSyn-based mouse models leads to improved pathology and motor outcomes (*Kim et al., 2015*; *Kim et al., 2018*). Our data demonstrate curli-dependent increases of inflammatory markers in both the intestine and brain, as well as acceleration of αSyn pathology, but do not determine which of these may be the primary driver of curli-mediated pathophysiology. Disentangling these complex relationships in future studies will define how pathologic signals from bacterial amyloids are transduced from the gut to the brain, via transneuronal spread of αSyn aggregates and/or an inflammatory cascade, and mechanisms of gut-to-brain signaling that contribute to motor impairment.

Synucleinopathy is linked to marked changes to the structure of the microbiome. Numerous studies have reported microbiome differences in persons with PD compared to unaffected individuals (*Hasegawa et al., 2015*; *Keshavarzian et al., 2015*; *Scheperjans et al., 2015*; *Unger et al., 2016*; *Bedarf et al., 2017*; *Hill-Burns et al., 2017*; *Hopfner et al., 2017*; *Li et al., 2017*; *Barichella et al., 2019*; *Lin et al., 2018*); however, examination of the gut microbiome during other

synucleinopathies, such as MSA or LBD are still in their infancy (*Engen et al., 2017*). Some reports have identified the family Enterobacteriaceae as enriched in PD compared to unaffected individuals (*Unger et al., 2016*; *Li et al., 2017*; *Barichella et al., 2019*). In those studies which performed correlation analysis between disease severity and microbiome composition, enrichment of Enterobacteriaceae is observed to be positively associated with worsened motor symptoms (*Scheperjans et al., 2015*; *Li et al., 2017*). To our knowledge, no study to date has identified differential abundance of *csgA* or curli-encoding genes specifically in human incidences, and only a single study to date has utilized metagenomic sequencing of the gut microbiome during PD (*Bedarf et al., 2017*). Despite recent advances defining microbiome changes in neurodegenerative diseases, a contributing role by gut bacteria to synucleinopathies in humans remains correlative (reviewed in *Sampson, 2019*). In experimental models, however, transplant of fecal microbiomes from PD patients into ASO mice results in greater motor deficits than microbiomes from healthy controls (*Sampson et al., 2016*), suggesting functional consequences to changes in gut microbial composition.

Although our findings herein are limited to a single transgenic animal mouse model, and similar pathologies are observed in aged rats and nematodes (*Chen et al., 2016*), it is possible that these observations are model specific. Non-amyloid contributions from diverse gut bacteria are also likely to occur and influence neurodegenerative outcomes. For instance, enrichment of the gut bacterium *Proteus mirabilis*, or intestinal administration of its purified LPS, impairs the dopaminergic system of mice and increases susceptibility to neurotoxins (*Choi et al., 2018*). Infection with Gram-negative bacteria, including *Citrobacter* sp. (a taxonomic relative of *E. coli*), can trigger a pathological process leading to neurodegenerative immune responses in the brain and loss of midbrain dopamine production in a PD-relevant mouse model (*Matheoud et al., 2019*). In addition, specific microbiome-derived metabolites promote microglia maturation (*Erny et al., 2015*) and enhance αSyn-dependent pathology in germ-free mice (*Sampson et al., 2016*). Conversely, specific microbial metabolites (*Blacher et al., 2019*) or fecal microbiome transplants (*Sun et al., 2018*) may provide protection from neurodegenerative insults.

While CsgA is one example of bacterially-produced amyloid, microbial amyloid formation in general may influence physiological processes with outcomes relevant for neurodegenerative disease (*Friedland and Chapman, 2017*). For example, the *Pseudomonas* sp. functional amyloid, FapC, may also accelerate αSyn aggregation in vitro (*Christensen et al., 2019*), and bacterial chaperones of CsgA modulate αSyn amyloidogenesis (*Evans et al., 2015*). More broadly, CsgA is observed to accelerate amyloid β aggregation in vitro (*Hartman et al., 2013*; *Perov et al., 2019*), as well as the disease-associated amyloids, islet amyloid polypeptide (IAPP) and semen enhancer of viral infection (SEVI) in vitro (*Hartman et al., 2013*), and serum amyloid A in mice (*Lundmark et al., 2005*). Emerging evidence in diverse animal models suggests that gut bacteria may modulate amyloid-driven diseases, not only in synucleinopathy as we and others describe, but Alzheimer's disease (*Harach et al., 2017*; *Dodiya et al., 2019*) and amyotrophic lateral sclerosis (ALS) as well (*Blacher et al., 2019*), providing justification for future human studies and revealing possible new targets for interventions that may prevent, slow, or halt amyloid formation and neurodegenerative disease.

Materials and methods

Key resources table

Reagent type (species) or resource	Designation	Source or reference	Identifiers	Additional information
Strain, strain background (*Mus musculus*)	Thy1- alpha-synuclein (Line 61), BDF1 background	*Rockenstein et al., 2002*	ASO (alpha-synuclein over-expressing)	With permission, UCSD
Strain, strain background (*Escherichia coli*)	Str. K12, MC4100	*Zhou et al., 2013*	WT (wild-type)	

Continued on next page

Continued

Reagent type (species) or resource	Designation	Source or reference	Identifiers	Additional information
Strain, strain background (*Escherichia coli*)	Str. K12, MC4100:Δ*csgBAC*	*Zhou et al., 2013*	Δ*csgBAC*	
Strain (*Escherichia coli*)	Str. K12, MC4100: CsgA:Q49A/N54A/ Q139A/N144A	*Wang and Chapman, 2008*	SlowGo	
Antibody	Anti-alpha synuclein, mouse monoclonal	BD	Cat#: 610787	(1:1000)
Antibody	Anti-pS129 alpha-synuclein, rabbit monoclonal	AbCam	Cat#: Ab51253	(1:1000)
Antibody	Anti-tyrosine hydroxylase, mouse monoclonal	Millipore	Cat#: MAB318	(1:1000)
Antibody	Anti-Iba1, rabbit	Wako	Cat#: 019–19741	(1:1000)
Antibody	Anti-aggregated alpha-synuclein, rabbit polyclonal	AbCam	Cat#: MJFR-14-6-4-2	(1:1000)
Antibody	Anti-mouse IgG-546, goat polyclonal	Life Technologies	Cat#: A-11003	(1:1000)
Antibody	Anti-rabbit IgG-546, goat polyclonal	Life Technologies	Cat#: A-11010	(1:1000)
Antibody	Anti-mouse IgG-488, goat polyclonal	Life Technologies	Cat#: A-11001	(1:1000)
Antibody	Anti-rabbit IgG-HRP, goat polyclonal	Cell Signaling	Cat#: 7074	(1:1000)
Peptide, recombinant protein	CsgA (N'-QYGGNN-C')	Bio-Synthesis, Inc; *Tükel et al., 2009*	CsgA	
Peptide, recombinant protein	N122A (N'QYGGNA-C')	Bio-Synthesis, Inc; *Tükel et al., 2009*	N122A	
Sequence-based reagent	16S rRNA: 5'-TCCTACGGGAG GCAGCAGT-3' and 5'-GGACTACCAGGG TATCTAATCCTGTT-3'	IDT	qPCR primer	PrimerBank
Sequence-based reagent	*rrsA:* 5'-AGTGATAAACTG GAGGAGGTG-3' and 5'-GGACTACGACG CACTTTATGAG-3'	IDT	qPCR primer	PrimerBank
Sequence-based reagent	*csgA:* 5'-ATGACGGTTAA ACAGTTCGG-3' and 5'-AGGAGTTAGAT GCAGTCTGG-3'	IDT	qPCR primer	PrimerBank
Sequence-based reagent	*gapdh:* 5'-CATGGCCTTCC GTGTTCCTA-3' and 5'-CCTGCTTCACCA CCTTCTTGAT-3'	IDT	qPCR primer	PrimerBank

Continued on next page

Reagent type (species) or resource	Designation	Source or reference	Identifiers	Additional information
Sequence-based reagent	*il6:* 5'-TAGTCCTTCCTA CCCCAATTTCC-3' and 5'-TTGGTCCTTAGC CACTCCTTC-3',	IDT	qPCR primer	PrimerBank
Sequence-based reagent	*TH:* 5'-CCAAGGTTCAT TGGACGGC-3' and 5'-CTCTCCTCGAAT ACCACAGCC-3'	IDT	qPCR primer	PrimerBank
Sequence-based reagent	*tnfa;* 5'-CCCTCACACTCA GATCATCTTCT-3' and 5'-GCTACGACAG TGGGCTACAG-3'	IDT	qPCR primer	PrimerBank

Animals

Male wild-type and Thy1-αSyn mice (Line 61, with permission from University of California, San Diego) were generated as described previously (*Rockenstein et al., 2002*; *Chesselet et al., 2012*; *Sampson et al., 2016*), through breeding female BDF1 background Thy1-αSyn mice to male BDF1 offspring generated via crossing female C57BL/6 with DBA/2 males (Charles River, Hollister, CA), and refreshing breeding pairs ~ 6 months. Germ-free (GF) Thy1-αSyn breeding pairs were generated via caesarian section and cross-fostered by GF Swiss-Webster dams. Conventionally colonized and mono-colonized animals were housed in autoclaved, ventilated, microisolator caging. GF animals were housed in open-top caging within flexible film isolators and maintained microbiologically sterile, confirmed via 16S rRNA PCR from fecal-derived DNA and culture of fecal pellets on Brucella blood agar or tryptic soy blood agar (Teknova, Hollister, CA) under anaerobic and aerobic conditions, respectively. Mono-colonized animals received ~10^8 cfu of the indicated bacterial strains in ~100 µL sodium bicarbonate buffer (5% w/v) at 5–6 weeks of age. Human microbiome colonized animals received ~100 µL 0.1 g/mL fecal extract from previously sampled healthy human donor (ENA Accession: PRJEB17694; Sample #: 10483.donor2.HC; MMA_008 [*Sampson et al., 2016*], California Institute of Technology's Institutional Review Board #15–0568- exempt), at 5–6 weeks of age. For mice mono-colonized with *E. coli* containing plasmid vectors for CsgA and CsgA:SlowGo, drinking water was supplemented with 50 µg/mL kanamycin (Sigma Aldrich, St Louis, MO). Human microbiome colonized mice were associated with WT or Δ*csgBAC* mutant *E. coli* at time of microbiota transplant. For epigallocatechin gallate (EGCG) treatment, animals received filter-sterilized EGCG (Sigma Aldrich) at 200 µg/mL in drinking water ad libitum beginning at 5–6 weeks of age. All animals received autoclaved food (LabDiet Laboratory Autoclavable Diet 5010, St Louis, MO) and water ad libitum, were maintained on the same 12 hr light-dark cycle, and housed in the same room of the facility. All animal husbandry and experiments were approved by the California Institute of Technology's Institutional Animal Care and Use Committee (IACUC), through protocol #1707.

Motor function assessment

Motor function was assessed similarly to previous studies (*Fleming et al., 2004*; *Sampson et al., 2016*), between hours 7 and 9 of the light phase, within a biosafety cabinet. Beam traversal and pole descent were performed first, followed by fecal output measurement. One day later, wirehang, adhesive removal and hindlimb scoring was performed. *Beam traversal-* A 1 m plexiglass beam consisting of four segments of 0.25 m in length (Stark's Plastics, Forest Park, OH) was constructed with consecutively thinner widths of 3.5, 2.5, 1.5, and 0.5 cm, with 1 cm overhangs placed 1 cm below the surface of the beam and the narrowest end placed into home cage. Animals were trained for two consecutive days before the first testing. On the first day of training, animals received one trial with the home cage positioned close to the widest segment, where the animal was placed, and guided the animals forward along the narrowing beam. Animals received two more trials with limited or no assistance to encourage forward movement and stability on the beam. On the second day of

training, animals were given three trials to traverse the beam, with little to no assistance. On the third day, animals were timed over three trials to traverse from the widest segment to the home cage. Time was measured from the placement of the animal's forelimbs onto the second segment until a forelimb reached the home cage. Score was averaged over three trials. *Pole descent*- A 0.5 m long pole, 1 cm in diameter, wrapped with non-adhesive shelf liner to facilitate the animals grip, was placed into the home cage, with animals removed and placed into fresh housing. Animals received 2 days of training to descend from the top of the pole and into the home cage. On the first day, animals received three trials to descend the pole. First animals were placed head-down ~1/3 the distance above the base, the second trial from ~2/3 the height, and on the third trial animals were placed at the top of the pole, head-down. The second day of training, animals were tasked with descending, head-down, from the top of the pole, three times. On the day of testing, animals were placed head-down on the top of the pole and timed beginning when the experimenter released the animal and ended when one hind-limb was placed on the pole base. Score was averaged over three trials. *Adhesive removal*- ¼" round adhesive labels (Avery, Glendale, CA) were placed on the nasal bridge. Animals were placed into their home cage (with cage mates removed into separate cage) and timed to completely remove the sticker. Animals were recorded over two trials, and averaged. *Hindlimb clasping reflex scoring*- Animals were gently lifted by the mid-section of the tail and observed over ~5–10 s (*Zhang et al., 2014*). Animals were assigned a score of 0, 1, 2, or 3. 0 was scored to animals that freely moved both their limbs and extended them outwards. A 1 was assigned to animals which clasped one hindlimb inward for the duration of the restraint or if both legs exhibited partial inward clasping. 2 was given if both legs clasped inward for the majority of the observation, but still exhibited some flexibility. A score of 3 was assigned if animals displayed complete rigidity of hindlimbs that immediately clasped inward and exhibited no signs of flexibility. For animals in *Figure 3—figure supplement 2G*, animals were scored twice on 2 consecutive days and the score averaged, the remainder were scored once. *Wirehang*- Animals were placed in the center of a 30 cm by 30 cm screen with 1 cm wide mesh. The screen was inverted head-over-tail and placed on supports ~ 40 cm above an open cage with deep bedding. Animals were timed until they released their grip or remained for 60 s, and the score from two trials averaged. *Fecal Output*- Animals were removed from their home cages and placed into a 12 cm x 25 cm translucent cylinder. Fecal pellets were counted every 5 min, cumulative over 15 min. *Principal component analysis*- PCA was performed using ClustVis web tool, with default settings and reversed axis for display (*Metsalu and Vilo, 2015*).

Bacterial strains, manipulations, and characterizations

Escherichia coli K12 str. MC4100 and the previously characterized isogenic deletion mutant of the *csgBAC* operon were cultured aerobically in YESCA media at 37°C (*Zhou et al., 2013*). Biofilm assays were performed via crystal violet staining of static culture at room temperature in YESCA as described previously (*Zhou et al., 2013*). Congo red staining was performed on YESCA agar following 2–3 days growth at room temperature as described previously (*Zhou et al., 2013*). Fecal bacterial DNA was isolated using QuickDNA Fecal/Soil Microbe Miniprep (Zymo Research, Irvine, CA). Fecal bacterial RNA was isolated using PowerMicrobiome RNA Isolation kit (MoBio, Carlsbad, CA) and cDNA generated via iScript cDNA Synthesis kit (BioRad, Hercules, CA). qPCR was performed with SybrGreen master mix (Applied Biosystems, Foster City, CA) on an AB7900ht instrument using the following primers: 16 s rRNA-5'-TCCTACGGGAGGCAGCAGT-3' and 5'-GGACTACCAGGGTA TCTAATCCTGTT-3'; *rrsA*-5'-AGTGATAAACTGGAGGAGGTG- 'and 5'-GGACTACGACGCACTTTA TGAG-3'; *csgA*- 5'-ATGACGGTTAAACAGTTCGG-3' and 5'-AGGAGTTAGATGCAGTCTGG-3'. *Bacteroides fragilis* str. NTCT9343 was cultured anaerobically in brain-heart infusion (BHI) broth at 37°C, and colonized into GF animals via oral gavage of ~10^8 cfu in 100 µL sodium bicarbonate buffer (5% w/v) at 5–6 weeks of age. Segmented filamentous bacteria were colonized via bedding transfer and co-housing within a mono-associated gnotobiotic isolator. Colonization was confirmed by PCR for SFB 16 s RNA. For growth curves, *E. coli* was first grown aerobically at 37°C overnight in BHI broth, and subcultured at 1:400 in BHI containing indicated concentrations of EGCG, in a 200 µL volume in a 96-well plate. Plates were incubated at 37°C aerobically, with orbital shaking in a BioTek Cytation 5 plate reader, and the optical density at 600 nm measured every hour. Endotoxin content was measured following overnight growth at 37°C, aerobically in BHI using the Pierce LAL Chromogenic Endotoxin kit (ThermoFisher, Pittsburgh, PA) according to manufacturer's instructions. LPS was

stained from lysates derived from identically grown bacterial cultures following separation on a 4–20% SDS-PAGE gel with Pro-Q Emerald 300 LPS stain kit (ThermoFisher), according to manufacturer's instructions.

α-Synuclein aggregation assays

Thioflavin T (ThT) assays-Freshly purified CsgA (both wild-type and 'SlowGo') and αSyn were diluted in 50 mM KPi (pH 7.3) to the molar concentrations indicated in each experiment. Samples were incubated in 96-well, black, flat bottom plates at 37°C with 20 μM ThT and 100 mM NaCl under continuous shaking conditions, along with a 1 mm glass bead for homogenous mixing. The ThT fluorescence intensity was recorded in 30 min interval using a Tecan plate reader (excitation: 438 nm; emission: 495 nm; cut-off: 475 nm). *TauK18 aggregation assay*- 50 μM of TauK18 fragment with heparin (TauK18:Heparin 4:1) was incubated with or without CsgA (2 μM) in 14 mM MES buffer pH 6.8 at 37°C with continuous shaking in 96-well, black, flat bottom plates. 2 mm beads and 20 μM ThT was added to all the wells. The ThT fluorescence was monitored with previously mentioned parameters after 30 min in FLUOstar omega plate reader (BMG Labtech). *Transmission electron microscopy*- Aliquots of CsgA and αSyn reactions were taken at indicated timepoints. Five microliters of sample was applied on glow-discharged carbon-coated grids, incubated for 1 min and washed with MilliQ water before staining with 1% uranyl acetate. Samples were imaged on Jeol electron microscope (JEOL-1400 plus). *Circular dichroism spectroscopy*- αSyn alone or with CsgA (in 20 mM KPi pH 7.3) were analyzed using a Jasco J-810 spectropolarimeter from 190 nm to 250 nm at 25°C immediately after purification and at indicated timepoints.

Synuclein pathology and inflammatory responses

CD11b enrichment- Animals were sedated with pentobarbital and perfused; whole brains were homogenized in PBS via passage through a 100 μm mesh filter, myelin debris were removed using magnetic separation with Myelin Removal Beads (Miltenyi Biotec, San Diego, CA), and subsequently CD11b positive enrichment performed similarly, via Microglia Microbeads (Miltenyi Biotec), according to manufacturer's instructions. Cells were immediately lysed in Trizol and RNA extracted with the DirectZol RNA extraction (Zymo Research). cDNA and qPCR performed as described above with primers- *gapdh*: 5'-CATGGCCTTCCGTGTTCCTA-3' and 5'-CCTGCTTCACCACCTTCTTGAT-3'; *il6*: 5'-TAGTCCTTCCTACCCCAATTTCC-3' and 5'-TTGGTCCTTAGCCACTCCTTC-3', *tyrosine hydroxylase*: 5'-CCAAGGTTCATTGGACGGC-3' and 5'-CTCTCCTCGAATACCACAGCC-3'; and *tnfa*; 5'-CCCTCACACTCAGATCATCTTCT-3' and 5'-gctacgacagtgggctacag-3'. *Synuclein imaging*- Perfused whole brains were dissected and fixed with 4% (w/v) paraformaldehyde. 50 μm sections were generated via vibratome. For proteinase-K resistant staining, free-floating sections were treated briefly with 5 μg/mL proteinase K (NEB, Ipswich, MA) and stained with anti-alpha synuclein (1:1000 mouse; #610787 BD, Franklin Lakes, NJ), pS129-synuclein staining utilized anti-pS129syn (1:1000 rabbit; #ab51253 AbCam, Cambridge, UK) and anti-tyrosine hydroxylase (1:1000 mouse; MAB318, Millipore, Burlington, MA). Sections were stained with secondary anti-mouse IgG-AF488 (1:1000, Life Technologies, Carlsbad, CA), anti-rabbit IgG-546 (1:1000, Life Technologies) and Neurotrace (Life Technologies), mounted with ProFade Diamond DAPI (Life Technologies) and imaged with a 20x objective on a Zeiss LSM800 confocal microscope. Sections corresponding to ~1500 μm from midline were counted manually for TH[+] cell bodies and pS129syn puncta in ImageJ software. *Microglia reconstructions*- Microglia were imaged and analyzed as previously described (*Erny et al., 2015*; *Sampson et al., 2016*). Thin sections prepared as above were stained with anti-Iba1 (1:1000 rabbit, Wako, Richmond, VA) and anti-rabbit IgG-AF546 (1:1000, Life Technologies). Z-stacks were imaged at 1 μm steps and analyzed using Imaris software. *ELISAs*- For TNFα and IL6 (eBioscience, San Diego, CA), αSyn (ThermoFisher), and dopamine (Eagle Biosciences, Nashua, NH) tissue homogenates were prepared in RIPA buffer containing protease inhibitor (ThermoFisher), and ELISA performed according to manufacturer's instructions with 100 μg of tissue. Multiplexed intestine (100 μg) and serum cytokine levels were measured on a Bio-Plex 200 using the Bio-Plex Mouse Cytokine 23-plex Assay (Biorad) according to manufacturer's instructions. *Dot blot*- Tissue homogenates were spotted onto 0.45 μm nitrocellulose membranes, in 1 μg/μL aliquots. Membranes were blocked with 5% dry skim milk in Tris-buffered saline and stained with anti-aggregated alpha-synuclein antibody (1:1000, MJFR-14-6-4-2, rabbit, AbCam) and anti-rabbit IgG-HRP (1:1000, Cell Signaling Technology,

Danvers, MA), and detected with Clarity chemiluminescence substrate (BioRad) on a BioRad GelDoc XR and densitometry performed.

Intestinal injections

Synthetic hexapeptides of CsgA (Nterm-QYGGNN-Cterm) and the non-amyloidogenic mutant N122A (Nterm-QYGGNA-Cterm) were purchased from Bio-Synthesis Inc (Lewisville, TX). Mice were anesthetized with isoflurane (1–4% vol/vol) and kept on a self-regulating heating pad throughout the procedure. A 10 µl Hamilton syringe fitted with a 36-gauge beveled needle was loaded with 30 µg of either hexapeptide in saline (9 µl total). Each animal was injected in three locations (both sides of pyloric antrum and duodenum [0.5 cm past the pyloric sphincter]; 3 µl each location) by inserting the needle tip bevel facing up into the intestine wall at a 15° angle. After injection, the abdominal muscle/peritoneal layer and skin were sutured separately, then mice returned to home cages. Mice were injected subcutaneously with buprenorphine SR (1 mg/kg) and monitored for 3 days for normal food and water consumption.

Statistics and data availability

Data were analyzed in GraphPad Prism, with the analysis indicated in each figure legend. Statistical output and numerical source data presented within the manuscript are available within the supplementary information included with this manuscript.

Additional information

Competing interests

Timothy R Sampson: has intellectual property pending in relationship to the content of this manuscript, US Patent App. 15/893,456 and 16/302,321. Matthew Chapman: a member of the Scientific Advisory Board of Axial Biotherapeutics. Sarkis K Mazmanian: has financial interest in Axial Biotherapeutics. Has intellectual property pending in relationship to the content of this manuscript, US Patent App. 15/893,456 and 16/302,321. The other authors declare that no competing interests exist.

Author contributions

Timothy R Sampson, Conceptualization, Investigation, Visualization; Collin Challis, Neha Jain, Anastasiya Moiseyenko, Mark S Ladinsky, Istvan Horvath, Investigation, Visualization; Gauri G Shastri, Brittany D Needham, Investigation; Taren Thron, Resources, Investigation; Justine W Debelius, Stefan Janssen, Formal analysis; Rob Knight, Viviana Gradinaru, Supervision; Pernilla Wittung-Stafshede, Matthew Chapman, Sarkis K Mazmanian, Conceptualization, Supervision

Author ORCIDs

Timothy R Sampson https://orcid.org/0000-0002-2486-8766
Stefan Janssen https://orcid.org/0000-0003-0955-0589
Pernilla Wittung-Stafshede https://orcid.org/0000-0003-1058-1964
Viviana Gradinaru http://orcid.org/0000-0001-5868-348X
Sarkis K Mazmanian https://orcid.org/0000-0003-2713-1513

Ethics

Animal experimentation: All animal husbandry and experiments were approved by the California Institute of Technology's Institutional Animal Care and Use Committee (IACUC) under protocol #1707.

Decision letter and Author response

Decision letter https://doi.org/10.7554/eLife.53111.sa1
Author response https://doi.org/10.7554/eLife.53111.sa2

Additional files

Supplementary files

• Transparent reporting form

Data availability

All data generated or analysed during this study are included in the manuscript and supporting files. Source data files and statistical output for all figures have been provided.

References

Barichella M, Severgnini M, Cilia R, Cassani E, Bolliri C, Caronni S, Ferri V, Cancello R, Ceccarani C, Faierman S, Pinelli G, Bellis G, Zecca L, Cereda E, Consolandi C, Pezzoli G. 2019. Unraveling gut Microbiota in Parkinson's disease and atypical parkinsonism. *Movement Disorders* **34**:396–405. DOI: https://doi.org/10.1002/mds.27581

Bedarf JR, Hildebrand F, Coelho LP, Sunagawa S, Bahram M, Goeser F, Bork P, Wüllner U. 2017. Functional implications of microbial and viral gut metagenome changes in early stage L-DOPA-naïve parkinson's disease patients. *Genome Medicine* **9**:39. DOI: https://doi.org/10.1186/s13073-017-0428-y, PMID: 28449715

Bieschke J, Russ J, Friedrich RP, Ehrnhoefer DE, Wobst H, Neugebauer K, Wanker EE. 2010. EGCG remodels mature alpha-synuclein and amyloid-beta fibrils and reduces cellular toxicity. *PNAS* **107**:7710–7715. DOI: https://doi.org/10.1073/pnas.0910723107, PMID: 20385841

Blacher E, Bashiardes S, Shapiro H, Rothschild D, Mor U, Dori-Bachash M, Kleimeyer C, Moresi C, Harnik Y, Zur M, Zabari M, Brik RB-Z, Kviatcovsky D, Zmora N, Cohen Y, Bar N, Levi I, Amar N, Mehlman T, Brandis A, et al.

2019. Potential roles of gut microbiome and metabolites in modulating ALS in mice. *Nature* **572**:474–480. DOI: https://doi.org/10.1038/s41586-019-1443-5

Braak H, Rüb U, Gai WP, Del Tredici K. 2003. Idiopathic Parkinson's disease: possible routes by which vulnerable neuronal types may be subject to neuroinvasion by an unknown pathogen. *Journal of Neural Transmission* **110**: 517–536. DOI: https://doi.org/10.1007/s00702-002-0808-2, PMID: 12721813

Brettschneider J, Del Tredici K, Lee VM, Trojanowski JQ. 2015. Spreading of pathology in neurodegenerative diseases: a focus on human studies. *Nature Reviews Neuroscience* **16**:109–120. DOI: https://doi.org/10.1038/nrn3887, PMID: 25588378

Cai Z-Y, Li X-M, Liang J-P, Xiang L-P, Wang K-R, Shi Y-L, Yang R, Shi M, Ye J-H, Lu J-L, Zheng X-Q, Liang Y-R. 2018. Bioavailability of tea catechins and its improvement. *Molecules* **23**:2346. DOI: https://doi.org/10.3390/molecules23092346

Chen SG, Stribinskis V, Rane MJ, Demuth DR, Gozal E, Roberts AM, Jagadapillai R, Liu R, Choe K, Shivakumar B, Son F, Jin S, Kerber R, Adame A, Masliah E, Friedland RP. 2016. Exposure to the functional bacterial amyloid protein curli enhances Alpha-Synuclein aggregation in aged Fischer 344 rats and *Caenorhabditis elegans*. *Scientific Reports* **6**:34477. DOI: https://doi.org/10.1038/srep34477, PMID: 27708338

Chesselet MF, Richter F, Zhu C, Magen I, Watson MB, Subramaniam SR. 2012. A progressive mouse model of Parkinson's disease: the Thy1-aSyn ("Line 61") mice. *Neurotherapeutics* **9**:297–314. DOI: https://doi.org/10.1007/s13311-012-0104-2, PMID: 22350713

Choi JG, Kim N, Ju IG, Eo H, Lim SM, Jang SE, Kim DH, Oh MS. 2018. Oral administration of Proteus mirabilis damages dopaminergic neurons and motor functions in mice. *Scientific Reports* **8**:1275. DOI: https://doi.org/10.1038/s41598-018-19646-x, PMID: 29352191

Chorell E, Andersson E, Evans ML, Jain N, Götheson A, Åden J, Chapman MR, Almqvist F, Wittung-Stafshede P. 2015. Bacterial chaperones CsgE and CsgC differentially modulate human α-Synuclein amyloid formation via transient contacts. *PLOS ONE* **10**:e0140194. DOI: https://doi.org/10.1371/journal.pone.0140194, PMID: 26465894

Christensen LFB, Jensen KF, Nielsen J, Vad BS, Christiansen G, Otzen DE. 2019. Reducing the amyloidogenicity of functional amyloid protein FapC increases its ability to inhibit α-Synuclein fibrillation. *ACS Omega* **4**:4029–4039. DOI: https://doi.org/10.1021/acsomega.8b03590, PMID: 31459612

Clinton LK, Blurton-Jones M, Myczek K, Trojanowski JQ, LaFerla FM. 2010. Synergistic interactions between A , Tau, and -Synuclein: Acceleration of Neuropathology and Cognitive Decline. *Journal of Neuroscience* **30**:7281–7289. DOI: https://doi.org/10.1523/JNEUROSCI.0490-10.2010

Colosimo C. 2011. Nonmotor presentations of multiple system atrophy. *Nature Reviews Neurology* **7**:295–298. DOI: https://doi.org/10.1038/nrneurol.2011.5, PMID: 21343894

Dodiya HB, Kuntz T, Shaik SM, Baufeld C, Leibowitz J, Zhang X, Gottel N, Zhang X, Butovsky O, Gilbert JA, Sisodia SS. 2019. Sex-specific effects of microbiome perturbations on cerebral aβ amyloidosis and microglia phenotypes. *The Journal of Experimental Medicine* **216**:1542–1560. DOI: https://doi.org/10.1084/jem.20182386, PMID: 31097468

Engen PA, Dodiya HB, Naqib A, Forsyth CB, Green SJ, Voigt RM, Kordower JH, Mutlu EA, Shannon KM, Keshavarzian A. 2017. The potential role of Gut-Derived inflammation in multiple system atrophy. *Journal of Parkinson's Disease* **7**:331–346. DOI: https://doi.org/10.3233/JPD-160991, PMID: 28234259

Erny D, Hrabě de Angelis AL, Jaitin D, Wieghofer P, Staszewski O, David E, Keren-Shaul H, Mahlakoiv T, Jakobshagen K, Buch T, Schwierzeck V, Utermöhlen O, Chun E, Garrett WS, McCoy KD, Diefenbach A, Staeheli P, Stecher B, Amit I, Prinz M. 2015. Host Microbiota constantly control maturation and function of microglia in the CNS. *Nature Neuroscience* **18**:965–977. DOI: https://doi.org/10.1038/nn.4030, PMID: 26030851

Evans ML, Chorell E, Taylor JD, Åden J, Götheson A, Li F, Koch M, Sefer L, Matthews SJ, Wittung-Stafshede P, Almqvist F, Chapman MR. 2015. The bacterial curli system possesses a potent and selective inhibitor of amyloid formation. *Molecular Cell* **57**:445–455. DOI: https://doi.org/10.1016/j.molcel.2014.12.025, PMID: 25620560

Fleming SM, Salcedo J, Fernagut PO, Rockenstein E, Masliah E, Levine MS, Chesselet MF. 2004. Early and progressive sensorimotor anomalies in mice overexpressing wild-type human alpha-synuclein. *Journal of Neuroscience* **24**:9434–9440. DOI: https://doi.org/10.1523/JNEUROSCI.3080-04.2004, PMID: 15496679

Forsyth CB, Shannon KM, Kordower JH, Voigt RM, Shaikh M, Jaglin JA, Estes JD, Dodiya HB, Keshavarzian A. 2011. Increased intestinal permeability correlates with sigmoid mucosa alpha-synuclein staining and endotoxin exposure markers in early Parkinson's disease. *PLOS ONE* **6**:e28032. DOI: https://doi.org/10.1371/journal.pone.0028032, PMID: 22145021

Friedland RP, Chapman MR. 2017. The role of microbial amyloid in neurodegeneration. *PLOS Pathogens* **13**: e1006654. DOI: https://doi.org/10.1371/journal.ppat.1006654, PMID: 29267402

Fung TC, Olson CA, Hsiao EY. 2017. Interactions between the Microbiota, immune and nervous systems in health and disease. *Nature Neuroscience* **20**:145–155. DOI: https://doi.org/10.1038/nn.4476, PMID: 28092661

Gallo PM, Rapsinski GJ, Wilson RP, Oppong GO, Sriram U, Goulian M, Buttaro B, Caricchio R, Gallucci S, Tükel Ç. 2015. Amyloid-DNA composites of bacterial biofilms stimulate autoimmunity. *Immunity* **42**:1171–1184. DOI: https://doi.org/10.1016/j.immuni.2015.06.002, PMID: 26084027

Harach T, Marungruang N, Duthilleul N, Cheatham V, Mc Coy KD, Frisoni G, Neher JJ, Fåk F, Jucker M, Lasser T, Bolmont T. 2017. Reduction of abeta amyloid pathology in APPPS1 transgenic mice in the absence of gut Microbiota. *Scientific Reports* **7**:41802. DOI: https://doi.org/10.1038/srep41802, PMID: 28176819

Hartman K, Brender JR, Monde K, Ono A, Evans ML, Popovych N, Chapman MR, Ramamoorthy A. 2013. Bacterial curli protein promotes the conversion of PAP $_{248-286}$ into the amyloid SEVI: cross-seeding of dissimilar amyloid sequences . *PeerJ* **1**:e5. DOI: https://doi.org/10.7717/peerj.5

Hasegawa S, Goto S, Tsuji H, Okuno T, Asahara T, Nomoto K, Shibata A, Fujisawa Y, Minato T, Okamoto A, Ohno K, Hirayama M. 2015. Intestinal dysbiosis and lowered serum Lipopolysaccharide-Binding protein in Parkinson's Disease. *PLOS ONE* **10**:e0142164. DOI: https://doi.org/10.1371/journal.pone.0142164

Hill-Burns EM, Debelius JW, Morton JT, Wissemann WT, Lewis MR, Wallen ZD, Peddada SD, Factor SA, Molho E, Zabetian CP, Knight R, Payami H. 2017. Parkinson's disease and Parkinson's disease medications have distinct signatures of the gut microbiome. *Movement Disorders* **32**:739–749. DOI: https://doi.org/10.1002/mds.26942, PMID: 28195358

Holmqvist S, Chutna O, Bousset L, Aldrin-Kirk P, Li W, Björklund T, Wang ZY, Roybon L, Melki R, Li JY. 2014. Direct evidence of parkinson pathology spread from the gastrointestinal tract to the brain in rats. *Acta Neuropathologica* **128**:805–820. DOI: https://doi.org/10.1007/s00401-014-1343-6, PMID: 25296989

Hopfner F, Künstner A, Müller SH, Künzel S, Zeuner KE, Margraf NG, Deuschl G, Baines JF, Kuhlenbäumer G. 2017. Gut Microbiota in parkinson disease in a northern german cohort. *Brain Research* **1667**:41–45. DOI: https://doi.org/10.1016/j.brainres.2017.04.019, PMID: 28506555

Hui KY, Fernandez-Hernandez H, Hu J, Schaffner A, Pankratz N, Hsu N-Y, Chuang L-S, Carmi S, Villaverde N, Li X, Rivas M, Levine AP, Bao X, Labrias PR, Haritunians T, Ruane D, Gettler K, Chen E, Li D, Schiff ER, et al. 2018. Functional variants in the *LRRK2* gene confer shared effects on risk for Crohn's disease and Parkinson's disease . *Science Translational Medicine* **10**:eaai7795. DOI: https://doi.org/10.1126/scitranslmed.aai7795

Johnson ME, Stecher B, Labrie V, Brundin L, Brundin P. 2019. Triggers, facilitators, and aggravators: redefining Parkinson's Disease Pathogenesis. *Trends in Neurosciences* **42**:4–13. DOI: https://doi.org/10.1016/j.tins.2018.09.007

Jucker M, Walker LC. 2013. Self-propagation of pathogenic protein aggregates in neurodegenerative diseases. *Nature* **501**:45–51. DOI: https://doi.org/10.1038/nature12481, PMID: 24005412

Katorcha E, Makarava N, Lee YJ, Lindberg I, Monteiro MJ, Kovacs GG, Baskakov IV. 2017. Cross-seeding of prions by aggregated α-synuclein leads to transmissible spongiform encephalopathy. *PLOS Pathogens* **13**:e1006563. DOI: https://doi.org/10.1371/journal.ppat.1006563, PMID: 28797122

Keshavarzian A, Green SJ, Engen PA, Voigt RM, Naqib A, Forsyth CB, Mutlu E, Shannon KM. 2015. Colonic bacterial composition in Parkinson's disease. *Movement Disorders* **30**:1351–1360. DOI: https://doi.org/10.1002/mds.26307, PMID: 26179554

Killinger BA, Madaj Z, Sikora JW, Rey N, Haas AJ, Vepa Y, Lindqvist D, Chen H, Thomas PM, Brundin P, Brundin L, Labrie V. 2018. The vermiform appendix impacts the risk of developing Parkinson's disease. *Science Translational Medicine* **10**:eaar5280. DOI: https://doi.org/10.1126/scitranslmed.aar5280, PMID: 30381408

Kim C, Rockenstein E, Spencer B, Kim HK, Adame A, Trejo M, Stafa K, Lee HJ, Lee SJ, Masliah E. 2015. Antagonizing neuronal Toll-like receptor 2 prevents synucleinopathy by activating autophagy. *Cell Reports* **13**:771–782. DOI: https://doi.org/10.1016/j.celrep.2015.09.044, PMID: 26489461

Kim C, Spencer B, Rockenstein E, Yamakado H, Mante M, Adame A, Fields JA, Masliah D, Iba M, Lee HJ, Rissman RA, Lee SJ, Masliah E. 2018. Immunotherapy targeting toll-like receptor 2 alleviates neurodegeneration in models of synucleinopathy by modulating α-synuclein transmission and neuroinflammation. *Molecular Neurodegeneration* **13**:43. DOI: https://doi.org/10.1186/s13024-018-0276-2, PMID: 30092810

Kim S, Kwon SH, Kam TI, Panicker N, Karuppagounder SS, Lee S, Lee JH, Kim WR, Kook M, Foss CA, Shen C, Lee H, Kulkarni S, Pasricha PJ, Lee G, Pomper MG, Dawson VL, Dawson TM, Ko HS. 2019. Transneuronal propagation of pathologic α-Synuclein from the gut to the brain models Parkinson's Disease. *Neuron* **103**:627–641. DOI: https://doi.org/10.1016/j.neuron.2019.05.035, PMID: 31255487

Kishimoto Y, Zhu W, Hosoda W, Sen JM, Mattson MP. 2019. Chronic mild gut inflammation accelerates brain neuropathology and motor dysfunction in α-Synuclein mutant mice. *NeuroMolecular Medicine* **21**:239–249. DOI: https://doi.org/10.1007/s12017-019-08539-5, PMID: 31079293

Lam HA, Wu N, Cely I, Kelly RL, Hean S, Richter F, Magen I, Cepeda C, Ackerson LC, Walwyn W, Masliah E, Chesselet M-F, Levine MS, Maidment NT. 2011. Elevated tonic extracellular dopamine concentration and altered dopamine modulation of synaptic activity precede dopamine loss in the striatum of mice overexpressing human α-synuclein. *Journal of Neuroscience Research* **89**:1091–1102. DOI: https://doi.org/10.1002/jnr.22611

Lambert JD, Lee MJ, Lu H, Meng X, Hong JJ, Seril DN, Sturgill MG, Yang CS. 2003. Epigallocatechin-3-gallate is absorbed but extensively glucuronidated following oral administration to mice. *The Journal of Nutrition* **133**:4172–4177. DOI: https://doi.org/10.1093/jn/133.12.4172, PMID: 14652367

Li R, Huang YG, Fang D, Le WD. 2004. Epigallocatechin Gallate inhibits lipopolysaccharide-induced microglial activation and protects against inflammation-mediated dopaminergic neuronal injury. *Journal of Neuroscience Research* **78**:723–731. DOI: https://doi.org/10.1002/jnr.20315, PMID: 15478178

Li W, Wu X, Hu X, Wang T, Liang S, Duan Y, Jin F, Qin B. 2017. Structural changes of gut Microbiota in Parkinson's disease and its correlation with clinical features. *Science China Life Sciences* **60**:1223–1233. DOI: https://doi.org/10.1007/s11427-016-9001-4, PMID: 28536926

Lin LC, Wang MN, Tseng TY, Sung JS, Tsai TH. 2007. Pharmacokinetics of (-)-epigallocatechin-3-gallate in conscious and freely moving rats and its brain regional distribution. *Journal of Agricultural and Food Chemistry* **55**:1517–1524. DOI: https://doi.org/10.1021/jf062816a, PMID: 17256961

Lin A, Zheng W, He Y, Tang W, Wei X, He R, Huang W, Su Y, Huang Y, Zhou H, Xie H. 2018. Gut Microbiota in patients with Parkinson's disease in southern China. *Parkinsonism & Related Disorders* **53**:82–88. DOI: https://doi.org/10.1016/j.parkreldis.2018.05.007, PMID: 29776865

Liu B, Fang F, Pedersen NL, Tillander A, Ludvigsson JF, Ekbom A, Svenningsson P, Chen H, Wirdefeldt K. 2017. Vagotomy and Parkinson disease: a swedish register-based matched-cohort study. *Neurology* **88**:1996–2002. DOI: https://doi.org/10.1212/WNL.0000000000003961, PMID: 28446653

Lundmark K, Westermark GT, Olsén A, Westermark P. 2005. Protein fibrils in nature can enhance amyloid protein A amyloidosis in mice: cross-seeding as a disease mechanism. *PNAS* **102**:6098–6102. DOI: https://doi.org/10.1073/pnas.0501814102, PMID: 15829582

Manfredsson FP, Luk KC, Benskey MJ, Gezer A, Garcia J, Kuhn NC, Sandoval IM, Patterson JR, O'Mara A, Yonkers R, Kordower JH. 2018. Induction of alpha-synuclein pathology in the enteric nervous system of the rat and non-human primate results in gastrointestinal dysmotility and transient CNS pathology. *Neurobiology of Disease* **112**:106–118. DOI: https://doi.org/10.1016/j.nbd.2018.01.008, PMID: 29341898

Matheoud D, Cannon T, Voisin A, Penttinen AM, Ramet L, Fahmy AM, Ducrot C, Laplante A, Bourque MJ, Zhu L, Cayrol R, Le Campion A, McBride HM, Gruenheid S, Trudeau LE, Desjardins M. 2019. Intestinal infection triggers parkinson's disease-like symptoms in Pink1$^{-/-}$ mice. *Nature* **571**:565–569. DOI: https://doi.org/10.1038/s41586-019-1405-y, PMID: 31316206

Mertsalmi TH, Aho VTE, Pereira PAB, Paulin L, Pekkonen E, Auvinen P, Scheperjans F. 2017. More than constipation - bowel symptoms in Parkinson's disease and their connection to gut microbiota. *European Journal of Neurology* **24**:1375–1383. DOI: https://doi.org/10.1111/ene.13398

Metsalu T, Vilo J. 2015. ClustVis: a web tool for visualizing clustering of multivariate data using principal component analysis and heatmap. *Nucleic Acids Research* **43**:W566–W570. DOI: https://doi.org/10.1093/nar/gkv468, PMID: 25969447

Perez-Pardo P, Dodiya HB, Engen PA, Forsyth CB, Huschens AM, Shaikh M, Voigt RM, Naqib A, Green SJ, Kordower JH, Shannon KM, Garssen J, Kraneveld AD, Keshavarzian A. 2019. Role of TLR4 in the gut-brain Axis in Parkinson's disease: a translational study from men to mice. *Gut* **68**:829–843. DOI: https://doi.org/10.1136/gutjnl-2018-316844, PMID: 30554160

Perov S, Lidor O, Salinas N, Golan N, Tayeb-Fligelman E, Deshmukh M, Willbold D, Landau M. 2019. Structural insights into curli CsgA Cross-β fibril architecture inspire repurposing of Anti-amyloid compounds as Anti-biofilm agents. *PLOS Pathogens* **15**:e1007978. DOI: https://doi.org/10.1371/journal.ppat.1007978, PMID: 31469892

Peter I, Dubinsky M, Bressman S, Park A, Lu C, Chen N, Wang A. 2018. Anti-Tumor necrosis factor therapy and incidence of parkinson disease among patients with inflammatory bowel disease. *JAMA Neurology* **75**:939–946. DOI: https://doi.org/10.1001/jamaneurol.2018.0605, PMID: 29710331

Poewe W, Seppi K, Tanner CM, Halliday GM, Brundin P, Volkmann J, Schrag AE, Lang AE. 2017. Parkinson disease. *Nature Reviews Disease Primers* **3**:17013. DOI: https://doi.org/10.1038/nrdp.2017.13, PMID: 28332488

Rahimi J, Kovacs GG. 2014. Prevalence of mixed pathologies in the aging brain. *Alzheimer's Research & Therapy* **6**:82. DOI: https://doi.org/10.1186/s13195-014-0082-1, PMID: 25419243

Ritz BR, Paul KC, Bronstein JM. 2016. Of pesticides and men: a California story of genes and environment in Parkinson's Disease. *Current Environmental Health Reports* **3**:40–52. DOI: https://doi.org/10.1007/s40572-016-0083-2, PMID: 26857251

Rockenstein E, Mallory M, Hashimoto M, Song D, Shults CW, Lang I, Masliah E. 2002. Differential neuropathological alterations in transgenic mice expressing alpha-synuclein from the platelet-derived growth factor and Thy-1 promoters. *Journal of Neuroscience Research* **68**:568–578. DOI: https://doi.org/10.1002/jnr.10231, PMID: 12111846

Sakakibara R, Doi H, Fukudo S. 2019. Lewy Body constipation. *Journal of the Anus, Rectum and Colon* **3**:10–17. DOI: https://doi.org/10.23922/jarc.2018-022, PMID: 31559362

Sampson TR, Debelius JW, Thron T, Janssen S, Shastri GG, Ilhan ZE, Challis C, Schretter CE, Rocha S, Gradinaru V, Chesselet MF, Keshavarzian A, Shannon KM, Krajmalnik-Brown R, Wittung-Stafshede P, Knight R, Mazmanian SK. 2016. Gut Microbiota regulate motor deficits and neuroinflammation in a model of Parkinson's Disease. *Cell* **167**:1469–1480. DOI: https://doi.org/10.1016/j.cell.2016.11.018, PMID: 27912057

Sampson T. 2019. The impact of indigenous microbes on Parkinson's Disease. *Neurobiology of Disease* **15**:104426. DOI: https://doi.org/10.1016/j.nbd.2019.03.014

Scheperjans F, Aho V, Pereira PA, Koskinen K, Paulin L, Pekkonen E, Haapaniemi E, Kaakkola S, Eerola-Rautio J, Pohja M, Kinnunen E, Murros K, Auvinen P. 2015. Gut Microbiota are related to Parkinson's disease and clinical phenotype. *Movement Disorders* **30**:350–358. DOI: https://doi.org/10.1002/mds.26069, PMID: 25476529

Serra DO, Mika F, Richter AM, Hengge R. 2016. The green tea polyphenol EGCG inhibits *E. coli* biofilm formation by impairing amyloid curli fibre assembly and downregulating the biofilm regulator CsgD via the σ(E)-dependent sRNA RybB. *Molecular Microbiology* **101**:136–151. DOI: https://doi.org/10.1111/mmi.13379, PMID: 26992034

Soldner F, Stelzer Y, Shivalila CS, Abraham BJ, Latourelle JC, Barrasa MI, Goldmann J, Myers RH, Young RA, Jaenisch R. 2016. Parkinson-associated risk variant in distal enhancer of α-synuclein modulates target gene expression. *Nature* **533**:95–99. DOI: https://doi.org/10.1038/nature17939, PMID: 27096366

Spires-Jones TL, Attems J, Thal DR. 2017. Interactions of pathological proteins in neurodegenerative diseases. *Acta Neuropathologica* **134**:187–205. DOI: https://doi.org/10.1007/s00401-017-1709-7, PMID: 28401333

Sun MF, Zhu YL, Zhou ZL, Jia XB, Xu YD, Yang Q, Cui C, Shen YQ. 2018. Neuroprotective effects of fecal Microbiota transplantation on MPTP-induced parkinson's disease mice: Gut microbiota, glial reaction and TLR4/TNF-α signaling pathway. *Brain, Behavior, and Immunity* **70**:48–60. DOI: https://doi.org/10.1016/j.bbi.2018.02.005, PMID: 29471030

Svensson E, Horváth-Puhó E, Thomsen RW, Djurhuus JC, Pedersen L, Borghammer P, Sørensen HT. 2015. Vagotomy and subsequent risk of Parkinson's disease. *Annals of Neurology* **78**:522–529. DOI: https://doi.org/10.1002/ana.24448, PMID: 26031848

Tükel C, Wilson RP, Nishimori JH, Pezeshki M, Chromy BA, Bäumler AJ. 2009. Responses to amyloids of microbial and host origin are mediated through Toll-like receptor 2. *Cell Host & Microbe* **6**:45–53. DOI: https://doi.org/10.1016/j.chom.2009.05.020, PMID: 19616765

Tursi SA, Tükel Çagla. 2018. Curli-Containing enteric biofilms inside and out: matrix composition, immune recognition, and disease implications. *Microbiology and Molecular Biology Reviews* **82**:00028-18. DOI: https://doi.org/10.1128/MMBR.00028-18

Uemura N, Yagi H, Uemura MT, Hatanaka Y, Yamakado H, Takahashi R. 2018. Inoculation of α-synuclein preformed fibrils into the mouse gastrointestinal tract induces lewy body-like aggregates in the brainstem via the vagus nerve. *Molecular Neurodegeneration* **13**:21. DOI: https://doi.org/10.1186/s13024-018-0257-5, PMID: 29751824

Unger MM, Spiegel J, Dillmann KU, Grundmann D, Philippeit H, Bürmann J, Faßbender K, Schwiertz A, Schäfer KH. 2016. Short chain fatty acids and gut Microbiota differ between patients with Parkinson's disease and age-matched controls. *Parkinsonism & Related Disorders* **32**:66–72. DOI: https://doi.org/10.1016/j.parkreldis.2016.08.019, PMID: 27591074

Van Den Berge N, Ferreira N, Gram H, Mikkelsen TW, Alstrup AKO, Casadei N, Tsung-Pin P, Riess O, Nyengaard JR, Tamgüney G, Jensen PH, Borghammer P. 2019. Evidence for bidirectional and trans-synaptic parasympathetic and sympathetic propagation of alpha-synuclein in rats. *Acta Neuropathologica* **138**:535–550. DOI: https://doi.org/10.1007/s00401-019-02040-w, PMID: 31254094

Verbaan D, Marinus J, Visser M, van Rooden SM, Stiggelbout AM, van Hilten JJ. 2007. Patient-reported autonomic symptoms in parkinson disease. *Neurology* **69**:333–341. DOI: https://doi.org/10.1212/01.wnl.0000266593.50534.e8, PMID: 17646625

Vidakovic L, Singh PK, Hartmann R, Nadell CD, Drescher K. 2018. Dynamic biofilm architecture confers individual and collective mechanisms of viral protection. *Nature Microbiology* **3**:26–31. DOI: https://doi.org/10.1038/s41564-017-0050-1, PMID: 29085075

Vuong HE, Yano JM, Fung TC, Hsiao EY. 2017. The microbiome and host behavior. *Annual Review of Neuroscience* **40**:21–49. DOI: https://doi.org/10.1146/annurev-neuro-072116-031347, PMID: 28301775

Wang L, Magen I, Yuan PQ, Subramaniam SR, Richter F, Chesselet MF, Taché Y. 2012. Mice overexpressing wild-type human alpha-synuclein display alterations in colonic myenteric ganglia and defecation. *Neurogastroenterology & Motility* **24**:e425–e436. DOI: https://doi.org/10.1111/j.1365-2982.2012.01974.x, PMID: 22779732

Wang X, Chapman MR. 2008. Sequence determinants of bacterial amyloid formation. *Journal of Molecular Biology* **380**:570–580. DOI: https://doi.org/10.1016/j.jmb.2008.05.019, PMID: 18565345

Woerman AL, Stöhr J, Aoyagi A, Rampersaud R, Krejciova Z, Watts JC, Ohyama T, Patel S, Widjaja K, Oehler A, Sanders DW, Diamond MI, Seeley WW, Middleton LT, Gentleman SM, Mordes DA, Südhof TC, Giles K, Prusiner SB. 2015. Propagation of prions causing synucleinopathies in cultured cells. *PNAS* **112**:E4949–E4958. DOI: https://doi.org/10.1073/pnas.1513426112, PMID: 26286986

Zhang J, Saur T, Duke AN, Grant SG, Platt DM, Rowlett JK, Isacson O, Yao WD. 2014. Motor impairments, striatal degeneration, and altered dopamine-glutamate interplay in mice lacking PSD-95. *Journal of Neurogenetics* **28**:98–111. DOI: https://doi.org/10.3109/01677063.2014.892486, PMID: 24702501

Zhou Y, Smith DR, Hufnagel DA, Chapman MR. 2013. Experimental manipulation of the microbial functional amyloid called curli. *Methods in Molecular Biology* **966**:53–75. DOI: https://doi.org/10.1007/978-1-62703-245-2_4, PMID: 23299728